Membrane compartmentalization of mycobacterial peptidoglycan synthesis

Alam García-Heredia[1], Julia Puffal[2], Julius Judd[3] *, Todd A. Gray[3,4], Yasu S. Morita[1,2, †], M. Sloan Siegrist[1,2, †].

Affiliations:

[1] Molecular and Cellular Biology Graduate Program, University of Massachusetts, Amherst, MA 01003, USA.

[2] Department of Microbiology, University of Massachusetts, Amherst, MA 01003, USA.

[3] Division of Genetics, Wadsworth Center, New York State Department of Health, Albany, NY 12208, USA.

[4] Department of Biomedical Sciences, University at Albany, Albany, NY 12208, USA.

[*] Current address: Department of Molecular Biology and Genetics, Cornell University, Ithaca, NY 14853, USA.

[†] Corresponding author. Email: siegrist@umass.edu (M.S.S.); ymorita@microbio.umass.edu (Y.S.M.).

Abstract: Cell wall peptidoglycan, a mesh of polysaccharides crosslinked by short peptides, encases the bacterial cell and protects it from turgor pressure lysis. Peptidoglycan synthesis is an effective antibiotic target. Assembly of the biopolymer occurs in close association with the plasma membrane, but higher order organization of the process has not been described. In mycobacteria, intracellular membrane domains comprise biochemically and spatially distinct regions within the conventional plasma membrane. We find that lipid-linked peptidoglycan precursors are made in these domains and then trafficked to the conventional plasma membrane for insertion into the

cell wall. Disorganization of the membrane rapidly delocalizes and then halts peptidoglycan assembly. Our data show that membrane compartmentalization is an essential feature of mycobacterial cell wall biogenesis.

Main Text: Many antibiotics target peptidoglycan synthesis, a well-conserved pathway that spans the cytoplasm, plasma membrane and periplasm. The polyprenol-linked, disaccharide-pentapeptide monomer lipid II is completed by the glycosyltransferase MurG in the inner leaflet of the plasma membrane (Fig. 1A). Lipid II is then flipped to the outer leaflet by MurJ and integrated into the cell wall by membrane-bound transglycosylases and transpeptidases from the penicillin-binding protein (PBP) and shape, elongation, division, and sporulation (SEDS) families (*1-4*).

The plasma membrane is a heterogeneous mixture of lipids and proteins. Mycobacteria, for example, have **i**ntracellular **m**embrane **d**omains (IMD, formerly called the PMf (*5*) for **p**lasma **m**embrane **f**ree of cell wall) that are separable from the conventional plasma membrane (designated the PM-CW, for **p**lasma **m**embrane tightly associated with **c**ell **w**all) by sucrose density gradient fractionation. The proteome and lipidome of IMD are distinct from PM-CW (*5, 6*). While PM-CW-resident proteins localize along the perimeter of live mycobacteria, IMD-resident proteins localize along sidewall but are enriched adjacent to sites of polar cell elongation (*6, 7*).

Our proteomics analysis indicated that MurG is present in the IMD while sequentially-acting PBPs preferentially associate with the PM-CW (*6*). We also observed *in situ* that the subpolar enrichment of MurG-RFP resembles that of the validated IMD marker mCherry-GlfT2 or GlfT2-GFP (*6, 8*) but that nascent cell wall at

47 the mycobacterial poles primarily abuts rather than colocalizes with mCherry-GlfT2 (*7*).
48 These observations suggest that lipid II synthesis is biochemically and spatially
49 segregated from the subsequent steps of cell wall assembly (Fig. 1A).

50 We expressed a functional MurG-Dendra2 fusion in *Mycobacterium smegmatis*
51 (Fig. S1) and assayed its distribution in membrane fractions that had been separated by
52 density gradient (Fig. 1B). The fusion to MurG, a peripheral membrane protein, was
53 enriched in both the cytoplasmic and IMD membrane fractions (Fig. 1C; Fig. S2),
54 recapitulating the association predicted for the native protein (*6*). In intact cells, polar
55 enrichment of MurG-Dendra2 was coincident with that of mCherry-GlfT2 (Fig. 1D). The
56 spatial relationship between the proteins was similar to that of MurG-RFP and GlfT2-
57 GFP (*8*), suggesting that it is independent of the fluorescent protein tag.

58 The association of MurG with the IMD, but not with the PM-CW, implied that the
59 membrane domain is the site of lipid II synthesis. We refined an *in vitro* D-amino acid
60 exchange assay to detect lipid-linked peptidoglycan precursors from *M. smegmatis*
61 membrane fractions (Fig. 2A; *9, 10*). In wildtype cells, we detected biotinylated
62 molecules in both the IMD and PM-CW (Fig. 2B; Fig. S2). We hypothesized that the
63 labeled species comprised precursors in the inner leaflet of the plasma membrane as
64 well as lipid II that had been flipped to the outer leaflet. We, and others, have shown
65 that depletion of MurJ results in an accumulation of biotinylated precursors (*10, 11*; Fig.
66 S3). By performing the D-amino acid exchange reaction on membrane fractions, we
67 found that precursors accumulate in the IMD (Fig. 2B; Fig. S2). These results suggest
68 that lipid II is made in the IMD and transferred to the PM-CW in a MurJ-dependent
69 manner.

70 PBPs and SEDS proteins incorporate lipid II into peptidoglycan. Given the
71 trafficking of precursors from the IMD to the PM-CW (Fig. 2B) and the association of cell
72 wall fragments specifically with the PM-CW (*5*), we hypothesized that extracellular,
73 peptidoglycan-acting enzymes function in the PM-CW. While our proteomics did not
74 detect SEDS proteins, our PM-CW dataset was enriched for all of the known
75 mycobacterial PBPs (*6*). Fluorescent derivatives of β-lactam antibiotics such as Bocillin-
76 FL bind covalently to PBPs and can be used to image transpeptidase-active enzymes in
77 both polyacrylamide gels and intact cells. We incubated membrane fractions from
78 wildtype *M. smegmatis* with Bocillin-FL and identified fluorescent proteins in the PM-CW
79 but not the IMD (Fig. 2B; Fig. S2). As expected for PBPs, the signal from these bands
80 was diminished by pre-treatment with the β-lactam ampicillin (Fig. S4). We focused on
81 characterizing PonA1, a bifunctional transglycosylase/transpeptidase that is essential
82 for *M. smegmatis* growth (*12, 13*). Depletion of PonA1 (*12*) resulted in the loss of the
83 highest molecular fluorescent band (Fig. S4), confirming that this protein is present and
84 active specifically in the PM-CW (Fig. 2B). We next expressed a functional PonA1-
85 mRFP fusion in *Mycobacterium smegmatis* (*13*) and found that it was more evenly
86 distributed around the cell perimeter than MurG-Dendra2, and in a manner similar to the
87 functional PM-CW marker PimE-GFP (Fig. 2C, Fig. S5; *6*). Together, our data show that
88 MurG and PonA1 occupy spatially distinct compartments along the pathway of
89 peptidoglycan synthesis.
90 Based on our biochemical data, we hypothesized that lipid II incorporation into
91 the cell wall is laterally segregated from its synthesis. We previously showed that
92 alkynyl and azido D-amino acid dipeptides (*14*) incorporate into lipid-linked

93 peptidoglycan precursors in *M. smegmatis* (*10*) and that metabolic labeling with alkynyl
94 dipeptide (alkDADA or EDA-DA) is most intense in regions adjacent to the IMD marker
95 mCherry-GlfT2 (*7*). We labeled MurG-Dendra2-expressing *M. smegmatis* with alkDADA
96 for ~1% of generation time and detected the presence of the alkyne by copper-
97 catalyzed azide-alkyne cycloaddition (CuAAC; Fig 2D; *10*). To tune our detection for
98 extracellular alkynes present in lipid II and newly-polymerized cell wall, we selected
99 picolyl azide-Cy3 as our label because the localized charge on the sulfonated cyanine
100 dye confers poor membrane permeability (*15*). Using this optimized protocol, we
101 observed nascent peptidoglycan deposition at the polar tip, whereas MurG-Dendra2
102 was more posterior (Fig. 2D). Our data support a model in which lipid II synthesis is
103 laterally and biochemically partitioned from the ensuing steps of peptidoglycan
104 assembly.

105 In the Gram-positive bacterium *Bacillus subtilis*, MurG associates with **r**egions of
106 **i**ncreased **f**luidity (RIFs) in the plasma membrane that are marked by the accumulation
107 of certain lipophilic fluorescent dyes (*16*). Benzyl alcohol has been used to disperse
108 plasma membrane domains in plant, animal and bacterial cells, including *B. subtilis*
109 RIFs (*16-18*). Mycobacteria are also Gram-positive but have a second 'myco'
110 membrane that is covalently attached to the cell wall. We found that benzyl alcohol did
111 not alter labeling by NalkTMM or OalkTMM (Fig. S6), which respectively incorporate into
112 the noncovalent and covalent mycolates of the mycomembrane (*19*). It did, however,
113 alter the distribution of FM4-64 (Fig. S7), a dye used previously to label the plasma
114 membrane (*20*), and altered glycolipid abundance in the IMD (Fig. S8). MurG-Dendra2
115 was also notably less enriched in the IMD following benzyl alcohol treatment (Fig. 1C)

116 and, in live cells, at the cell poles (Fig. 3A). By contrast benzyl alcohol produced subtle
117 changes in the distribution of active PBPs (Fig. 2B), although PonA1 shifted toward the
118 poles in live cells (Fig. 3A). Disruption of plasma membrane organization by benzyl
119 alcohol was accompanied by delocalization of cell wall assembly within 5 min (Fig. S9)
120 as well as an overall reduction in synthesis (Fig. 3B, Figs. S9) and halt in cell elongation
121 (Fig. S6). The phenotypes were reversible: we recovered viable, peptidoglycan-
122 synthesizing cells following benzyl alcohol washout (Figs. S10). These data suggest
123 that membrane partitioning is an essential feature of both peptidoglycan synthesis and
124 cell growth in *M. smegmatis*.

125 We find that benzyl alcohol also inhibits cell wall assembly in *B. subtilis* (Fig. 3C),
126 demonstrating that plasma membrane architecture may optimize peptidoglycan
127 biogenesis in bacterial phyla with divergent cell envelope structures and modes of
128 growth. Moreover, our previous work suggests that the biosynthetic pathways for
129 phosphatidylethanolamine, a major phospholipid of mycobacterial plasma membrane,
130 phosphatidylinositol mannoside, a cell envelope glycolipid, and menaquinone, the
131 primary lipid electron carrier of the mycobacterial respiratory chain, are partitioned
132 across the IMD and PM-CW (*5, 6, 21*). In the absence of a standard set of membrane-
133 bound organelles, plasma membrane compartmentalization may be a general bacterial
134 strategy for organizing pathways with lipid-linked intermediates and enzymes.

135 **References and Notes:**

136 1. C. L. Gee *et al.*, A phosphorylated pseudokinase complex controls cell wall
137 synthesis in mycobacteria. *Sci Signal* **5**, ra7 (2012).

138 2. A. J. Meeske *et al.*, SEDS proteins are a widespread family of bacterial cell wall
139 polymerases. *Nature* **537**, 634-638 (2016).
140 3. K. Emami *et al.*, Corrigendum: RodA as the missing glycosyltransferase in
141 *Bacillus subtilis* and antibiotic discovery for the peptidoglycan polymerase
142 pathway. *Nature Microbiology* **2**, 17019 (2017).
143 4. D. Arora *et al*., The transpeptidase PbpA and non-canonical transglycosylase
144 RodA of Mycobacterium tuberculosis play important roles in regulating bacterial
145 cell lengths. *J Biol Chem*, jbc. M117. 811190 (2018).
146 5. Y. S. Morita *et al.*, Compartmentalization of lipid biosynthesis in mycobacteria. *J*
147 *Biol Chem* **280**, 21645-21652 (2005).
148 6. J. M. Hayashi *et al.*, Spatially distinct and metabolically active membrane domain
149 in mycobacteria. *Proc Natl Acad Sci U S A* **113**, 5400-5405 (2016).
150 7. J. M. Hayashi *et al.*, Stress-Induced Reorganization of the Mycobacterial
151 Membrane Domain. *mBio* **9**, (2018).
152 8. X. Meniche *et al.*, Subpolar addition of new cell wall is directed by DivIVA in
153 mycobacteria. *Proc Natl Acad Sci U S A* **111**, E3243-3251 (2014).
154 9. Y. Qiao *et al.*, Detection of lipid-linked peptidoglycan precursors by exploiting an
155 unexpected transpeptidase reaction. *J Am Chem Soc* **136**, 14678-14681 (2014).
156 10. A. García-Heredia *et al.*, Peptidoglycan precursor synthesis along the sidewall of
157 pole-growing mycobacteria. *eLife* **7**, (2018).
158 11. Y. Qiao *et al.*, Lipid II overproduction allows direct assay of transpeptidase
159 inhibition by beta-lactams. *Nat Chem Biol* **13**, 793-798 (2017).

160 12. E. C. Hett *et al*., Interaction and modulation of two antagonistic cell wall enzymes
161 of mycobacteria. *PLoS Pathog* **6**, e1001020 (2010).
162 13. K. J. Kieser *et al.*, Phosphorylation of the peptidoglycan synthase PonA1 governs
163 the rate of polar elongation in mycobacteria. *PLoS Pathog* **11**, e1005010 (2015).
164 14. G. W. Liechti *et al.*, A new metabolic cell-wall labelling method reveals
165 peptidoglycan in *Chlamydia trachomatis*. *Nature* **506**, 507-510 (2014).
166 15. N. J. Yang, M. J. Hinner, Getting across the cell membrane: an overview for
167 small molecules, peptides, and proteins. *Methods in Molecular Biology (Clifton,*
168 *N.J.)* **1266**, 29-53 (2015).
169 16. A. Muller *et al.*, Daptomycin inhibits cell envelope synthesis by interfering with
170 fluid membrane microdomains. *Proc Natl Acad Sci U S A* **113**, E7077-e7086
171 (2016).
172 17. B. L. Orvar *et al*., Early steps in cold sensing by plant cells: the role of actin
173 cytoskeleton and membrane fluidity. *The Plant Journal* **23**, 785-794 (2000).
174 18. E. Nagy *et al.*, Hyperfluidization-coupled membrane microdomain reorganization
175 is linked to activation of the heat shock response in a murine melanoma cell line.
176 *Proc Natl Acad Sci U S A* **104**, 7945-7950 (2007).
177 19. H. N. Foley *et al*., Bioorthogonal chemical reporters for selective in situ probing of
178 mycomembrane components in mycobacteria. *Angewandte Chemie* **128**, 2093-
179 2097 (2016).
180 20. X. Zhou *et al.*, Sequential assembly of the septal cell envelope prior to V
181 snapping in *Corynebacterium glutamicum*. *Nature Chemical Biology*, 1 (2019).

182 21. J. Puffal *et al.*, Demethylmenaquinone Methyl Transferase Is a Membrane
183 Domain-Associated Protein Essential for Menaquinone Homeostasis in
184 *Mycobacterium smegmatis*. *Frontiers in Microbiology* **9**, 3145 (2018).
185 22. Y. S. Morita *et al.*, PimE is a polyprenol-phosphate-mannose-dependent
186 mannosyltransferase that transfers the fifth mannose of phosphatidylinositol
187 mannoside in mycobacteria. *Journal of Biological Chemistry*, (2006).
188 23. C. B. Sena *et al.*, Controlled expression of branch-forming mannosyltransferase
189 is critical for mycobacterial lipoarabinomannan biosynthesis. *Journal of Biological*
190 *Chemistry*, M109. 077297 (2010).
191 24. J. Schindelin *et al.*, Fiji: an open-source platform for biological-image analysis.
192 *Nature Methods* **9**, 676-682 (2012).
193 25. A. Paintdakhi *et al.*, Oufti: an integrated software package for high-accuracy,
194 high-throughput quantitative microscopy analysis. *Mol Microbiol* **99**, 767-777
195 (2016).
196

197 **Acknowledgments:** We are grateful to Drs. James Chambers and Amy Burnside for
198 microscopy and flow cytometry guidance, Drs. Eric Strieter and Jiaan Liu and Ms. Sylvia
199 Rivera for technical assistance. We also thank Drs. Hesper Rego and Eric Rubin for
200 ponA1-mRFP, and Dr. Christopher Sassetti for the MurJ and MurG depletion strains.
201 We thank Dr. Benjamin Swarts for providing the OalkTMM and NalkTMM probes.
202 **Funding:** Research was supported by funds from the National Institutes of Health (NIH)
203 under awards U01CA221230 and NIH DP2 AI138238 (M.S.S.) and R03 AI140259-01
204 (Y.S.M.), and R01 AI097191 (J.J. and T.A.G.). A.G.-H. was supported by an Honors

205 Fellowship from Universidad Autónoma de Nuevo León. J.P. is a recipient of the
206 Science Without Boarders Fellowship from CAPES-Brazil (0328-13-8). **Author**
207 **contributions:** Conceptualization: M.S.S., Y.S.M., A.G.-H. Formal analysis: A.G.-H.
208 Resources: M.S.S., Y.S.M., T.A.G. and J.J. Writing, review and editing: M.S.S., A.G.-
209 H.,Y.S.M., J.P., T.A.G. and J.J. **Competing interests:** Authors declare no competing
210 interests. **Data and materials availability:** All data are available in the main text or the
211 supplementary materials.
212

213 **Supplementary Materials:**
214 Materials and Methods
215 Figures S1-S10
216 Tables S1
217

218 **Fig. 1.** MurG is enriched in the IMD. (A) Membrane-bound steps of peptidoglycan
219 synthesis with hypothesized partitioning into the IMD and PM-CW. NAM, N-
220 acetylmuramic acid; NAG, N-acetylglucosamine; circles, amino acids: light green, L-ala;
221 red, D-glu; deep blue, diaminopimelic acid; yellow, D-ala. (B) Plasma membrane
222 fractionation. Bacteria are lysed by nitrogen cavitation and cell lysate is sedimented on
223 a sucrose density gradient. (C) Lysates from MurG-Dendra2-expressing *M. smegmatis*
224 were fractionated as in (B) and separated by SDS-PAGE. Protein detected by in-gel
225 fluorescence. Incubation of bacteria with 100 mM benzyl alcohol (BA) for 1 hour
226 decreased the enrichment of MurG-Dendra2 in the IMD. (D) *M. smegmatis*
227 coexpressing MurG-Dendra2 and mCherry-GlfT2 was imaged by structured illumination

228 microscopy (SIM-E, left). Fluorescence distribution of the fusion proteins from 59 cells
229 was quantitated from parallel conventional fluorescence microscopy (right). Signal was
230 normalized to the length and total fluorescence intensity of the cell. Cells were oriented
231 such that the brighter pole is on the right hand side of the graph. a.u., arbitrary units,
232 scalebar 5 μm.
233
234 **Fig. 2.** Lipid II is synthesized in the IMD and trafficked to the PM-CW. (A) Detection of
235 lipid-linked peptidoglycan precursors from organic extracts of *M. smegmatis* membrane
236 fractions. Terminal D-alanines (yellow) of endogenous precursors are exchanged for
237 biotin-D-lysine (BDL; pink) via purified *S. aureus* PBP4. Biotinylated species are
238 detected by blotting with streptavidin-HRP. (B) Detection of peptidoglycan precursors
239 and PonA1 activity from density gradient fractions. Precursors are in both the IMD and
240 PM-CW in wildtype *M. smegmatis* but accumulate in the IMD upon MurJ depletion (*10*).
241 PonA1 binds Bocillin-FL in the PM-CW before or after 1 hour of 100 mM benzyl alcohol
242 treatment. Wildtype *M. smegmatis* membrane fractions (50 μg/mL of total protein each)
243 were incubated with 40 μM Bocillin-FL and separated by SDS-PAGE. Active PBPs
244 detected by in-gel fluorescence in PM-CW. PonA1 was identified in Fig. S3. (C) SIM-E
245 of *M. smegmatis* coexpressing PonA1-mRFP and PimE-GFP, scalebar 5 μm. (D) Top,
246 metabolic labeling of mycobacterial cell wall synthesis (*10*). Bottom, *M. smegmatis*
247 expressing MurG-Dendra2 were incubated with alkDADA for 2 min (~1% generation).
248 Surface-exposed alkynes on fixed cells were detected by CuAAC with picolyl azide-Cy3
249 (*10*). Cells imaged by SIM-E, scalebar 5 μm.
250

251 **Fig. 3.** Perturbation of plasma membrane organization disrupts peptidoglycan
252 biogenesis. (A) *M. smegmatis* coexpressing PonA1-mRFP and MurG-Dendra2 were
253 imaged +/- benzyl alcohol by SIM-E (left). Fluorescence distribution of the fusion
254 proteins from 42<n<56 cells was quantitated from parallel conventional fluorescence
255 microscopy (right). Signal was normalized as Fig. 1D, scalebar 5 μm. (B) Wildtype *M.*
256 *smegmatis* +/- benzyl alcohol were incubated with both azido D-amino acid dipeptide
257 and mycomembrane probe OalkTMM (*10, 19*) for 15 min and fixed in 2% formaldehyde.
258 Alkynes and azides were detected by sequential CuAAC reactions with picolyl azide
259 TAMRA and alkyne carboxyrhodamine 110 (Click Chemistry Tools) labels with a wash
260 step between, scalebar 5 μm. (C) *B. subtilis* were exposed to indicated antibiotics or
261 benzyl alcohol for 10 min then incubated with alkDADA for an additional 5 min. Cells
262 were fixed and alkynes were detected by CuAAC with picolyl azide CR 110. MFI,
263 median fluorescence intensity obtained by flow cytometry. Experiments performed three
264 times in triplicate. Error bars, +/- standard deviation of biological replicates. ***, $p < 0.0005$; ****, $p < 0.00005$, Tukey multiple comparison test.
266

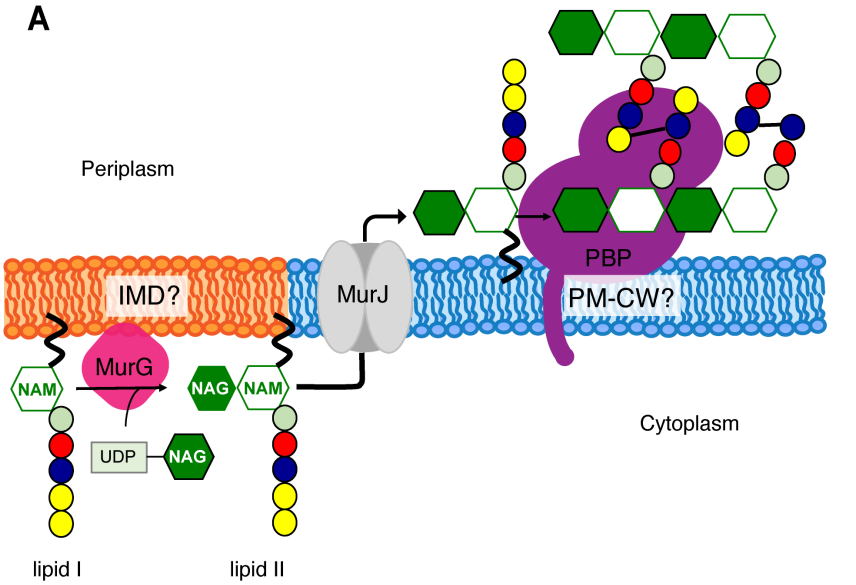
A
Periplasm
IMD?
MurG
NAM
NAG
NAM
UDP
NAG
MurJ
PBP
PM-CW?
Cytoplasm
lipid I
lipid II

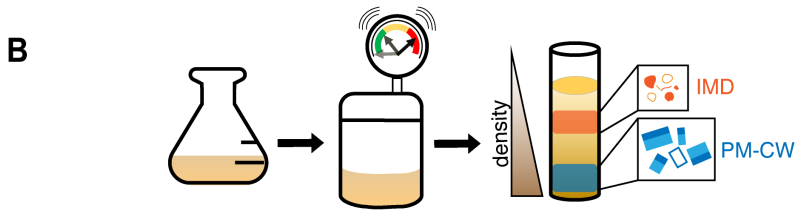
B
density
IMD
PM-CW

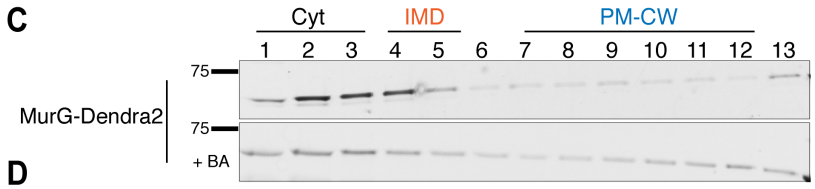
C
Cyt
IMD
PM-CW
1 2 3 4 5 6 7 8 9 10 11 12 13
75
MurG-Dendra2
75
+ BA

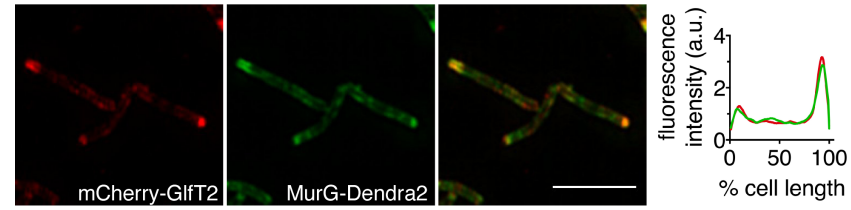
D
mCherry-GlfT2
MurG-Dendra2
fluorescence intensity (a.u.)
4
2
0
0
50
100
% cell length

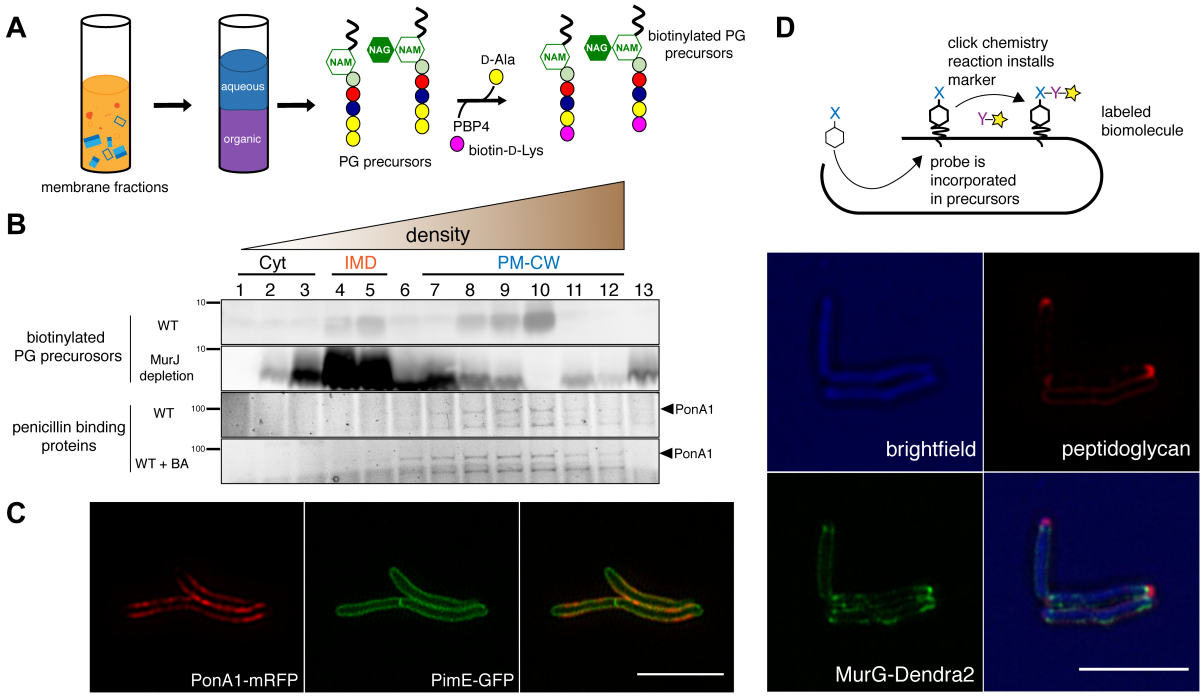
A
membrane fractions
aqueous
organic
NAM
NAG
NAM
PG precursors
D-Ala
PBP4
biotin-D-Lys
biotinylated PG precursors
B
density
Cyt
IMD
PM-CW
1 2 3 4 5 6 7 8 9 10 11 12 13
biotinylated PG precurosors
WT
MurJ depletion
penicillin binding proteins
WT
WT + BA
PonA1
PonA1
C
PonA1-mRFP
PimE-GFP
D
click chemistry reaction installs marker
X
X-Y
Y
labeled biomolecule
probe is incorporated in precursors
brightfield
peptidoglycan
MurG-Dendra2

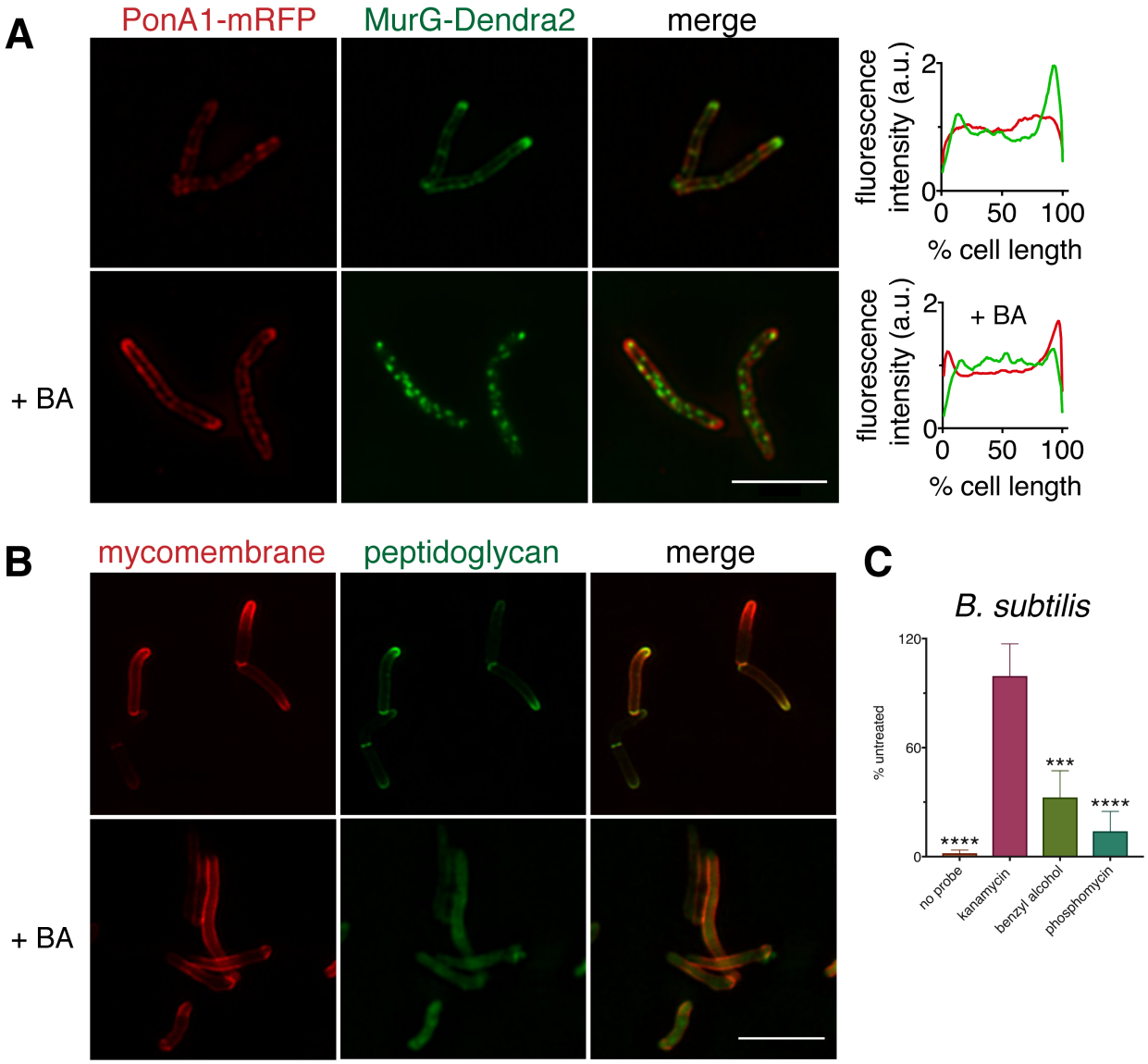
A
PonA1-mRFP
MurG-Dendra2
merge
+ BA
fluorescence intensity (a.u.)
2
0
0
50
100
% cell length
+ BA
fluorescence intensity (a.u.)
2
0
0
50
100
% cell length
B
mycomembrane
peptidoglycan
merge
+ BA
C
B. subtilis
120
60
0
% untreated
****
***
****
no probe
kanamycin
benzyl alcohol
phosphomycin